Journal of Alloys and Compounds 784 (2019) 1–7

Contents lists available at ScienceDirect

Journal of Alloys and Compounds

journal homepage: http://www.elsevier.com/locate/jalcom

Effect of solvent for tailoring the nanomorphology of multinary $CuCo_2S_4$ for overall water splitting and energy storage

Camila Zequine [a], Sanket Bhoyate [a], Fangzhou Wang [b], Xianglin Li [b], Khamis Siam [a], P.K. Kahol [c], Ram K. Gupta [a, d, *]

[a] Department of Chemistry, Pittsburg State University, Pittsburg, KS 66762, USA
[b] Department of Mechanical Engineering, University of Kansas, Lawrence, KS 66046, USA
[c] Department of Physics, Pittsburg State University, Pittsburg, KS 66762, USA
[d] Kansas Polymer Research Center, Pittsburg State University, Pittsburg, KS 66762, USA

ARTICLE INFO

Article history:
Received 6 October 2018
Received in revised form
31 December 2018
Accepted 2 January 2019
Available online 3 January 2019

Keywords:
Copper-cobalt oxide
Copper-cobalt sulfide
Mesoporous 3D flower-like nanostructures
Supercapacitor
Oxygen evolution
Hydrogen evolution

ABSTRACT

Tailoring the nanomorphology of electrochemically active materials could significantly affect their resultant catalytic and charge storage performance. In this study, the nanostructured morphology of multinary $CuCo_2O_4$ and $CuCo_2S_4$ was tuned using a different volume concentration of water and ethanol resulting in different nano-shapes maintaining similar crystal structure. The electrocatalytic performance was analyzed for all the synthesized samples as the hydrogen (HER) and oxygen evolution catalyst (OER). The HER and OER study for $CuCo_2S_4$ sample synthesized using ethanol required a low overpotential of 158 mV to reach 10 mA/cm^2 and 290 mV to achieve 20 mA/cm^2, respectively. Furthermore, the electrolyzer cell using symmetrical electrodes required a low overall cell potential of 1.66 V to achieve a current density of 10 mA/cm^2 and maintained stable performance for over 24 h, suggesting a promising bifunctional catalytic behavior. Furthermore, the synthesized samples were studied as electrodes for high-performance energy storage systems. The $CuCo_2S_4$ electrode showed an areal capacitance of 6.3 F/cm^2 (3190.8 F/g) at a current density of 2 mA/cm^2. The Ragone plot for the areal energy versus power density resulted to be 265 mWh/cm^2 (132 Wh/kg) and 11.9 W/cm^2 (5973 W/kg), respectively. Thus, from the overall study, it can be confirmed that tailoring morphology of nanostructured material such as $CuCo_2S_4$ could be a promising way for the advancement of energy generation and storage devices.

1. Introduction

Today's clean energy scenario focus on sustainable energy conversion and storage devices. Hydrogen and oxygen production through overall water splitting using electrocatalysis have shown a promising margin of research. Compared to conventional gasoline engines which convert chemical energy into heat and then to mechanical work (considering most of the energy is drained while conversion), hydrogen fuel cells provide direct conversion of chemical energy to electricity avoiding the thermal bottleneck. Moreover, they release water and little heat as byproduct contributing to environmental friendliness. Thus, producing hydrogen in an environment-friendly manner using water electrolysis with minimal thermodynamic overpotential loss is essential for their wide range applicability [1–5].

To meet current technological growth, multifunctional and smart material systems are required to be developed resulting in an efficient low-cost alternate for energy generation and storage. Copper-based multinary sulfides are an important class of inorganic metal sulfides due to following key aspects: (i) abundant availability, reduced cost and toxicity; (ii) excellent intrinsic functional properties such as notable charge carrier mobility with higher carrier concentration; and (iii) their morphological, compositional and stoichiometric tailoring ability [6]. This could allow its applicability in fields of photonics, biomedical, sensing, catalysis, and energy storage [7–9].

Tailoring the nano-morphology could result in the enhanced electrochemical performance of the electroactive materials. Bulk metal oxides and sulfides show inferior electrochemical performance due to limited conductivity and electroactive surface area [3,10]. Therefore, a thin film of nanostructured materials with the

* Corresponding author. Department of Chemistry, Pittsburg State University, Pittsburg, KS 66762, USA.
E-mail address: rgupta@pittstate.edu (R.K. Gupta).

https://doi.org/10.1016/j.jallcom.2019.01.012
0925-8388/

higher electrocatalytic surface area is preferred. Various morphologies for copper-based multinary metal oxides/sulfides such as rod-shaped, quasi-spherical, spherical, nanosheets, flower-like, nanograss and nano-belts have been synthesized using solution route to obtain enhanced performance [10–15]. Solvent-based synthesis could result in the facile tuning of nano-morphology. For example, Tang et al. studied the effect of solvents such as water, glycol, and glycerol, during synthesis of $CuCo_2S_4$ to obtain tuned porosity within the structure and observed the enhancement in charge storage capacity [16]. Similarly, significant effect over nano-morphology could be observed by using a different concentration of ethanol during synthesis.

Wei et al. have synthesized hierarchical $CuCo_2O_4$ for water splitting and supercapacitor applications [17]. The electrocatalytic activities of $CuCo_2O_4$ was improved by decorating carbon quantum dots over $CuCo_2O_4$. The effect of reaction temperature on the electrochemical properties of copper cobalt sulfide for supercapacitors was studied [18]. It was observed that the hydrothermal temperature is a crucial factor for the crystallinity, morphology and electrochemical performance of $CuCo_2S_4$. Chauhan et al. have used X-ray photoelectron spectroscopy and electron paramagnetic resonance to study the mechanics of enhanced performance of $CuCo_2S_4$ [19]. It was revealed that introduction of Cu into the Co_3S_4 lattice plays an active role in enhancing oxygen evolution and kinetics. Hierarchically structured $CuCo_2S_4$ nanowire was used as cost effective and efficient material for overall water splitting [20]. The fabricated electrolyzer required a low potential of 1.65 V to generate 100 mA/cm^2 3D mesoporous flower-like $CuCo_2S_4$/$CuCo_2O_4$ heterostructure as a cathode and graphene aerogel as anode was used for fabrication of an asymmetric supercapacitor [21]. The device delivered high energy density (33.2 Wh/kg) and power density (13.3 kW/kg).

In this study, we have synthesized copper-cobalt based multinary sulfide as an electrocatalyst for overall water splitting and energy storage supercapacitor. Nanocrystals of copper-cobalt oxide ($CuCo_2O_4$) and copper-cobalt sulfide ($CuCo_2S_4$) were synthesized using different volume concentration of water and ethanol as solvents. The varied concentration of solvents tailored the nano-morphology of $CuCo_2S_4$, resulting in superior electrocatalytic and charge storage performance. The $CuCo_2S_4$ electrode synthesized using ethanol showed a lower OER overpotential of 290 mV to achieve a current density of 20 mA/cm^2 and a lower HER overpotential of 158 mV to achieve a current density of 10 mA/cm^2. Further analysis of $CuCo_2S_4$ electrode as a supercapacitor electrode, showed high energy and power densities of 265 mWh/cm^2 and 11.9 W/cm^2, respectively. Thereby, an overall study on $CuCo_2S_4$ electrode proved that it could serve as a promising electrode material for multifunctional energy generation and storage devices.

2. Experimental details

The overall reaction scheme is summarized in Fig. 1. In the first step, copper cobalt oxide was synthesized using one pot hydrothermal method. This was carried out by dissolving 528 mg of $Co(NO_3)_2 \cdot 6H_2O$, 93.8 mg of $Cu(NO_3)_2 \cdot 3H_2O$ and 721 mg of urea in three solvent compositions. The compositions consist of 100 vol% water, 50/50 vol% water/ethanol, and 100 vol% ethanol, in a total of 34 ml. The dissolved mixtures were transferred to a Teflon autoclave reactor consisting pre-cleaned nickel foam. The reaction was carried out at 120 °C for 8 h. After completion of the reaction, the reactor was allowed to cool naturally. The resultant precipitate was washed several times with ethanol and dried overnight under vacuum at 80 °C before use. Similarly, the coated Ni-foams were washed several times with ethanol and dried under overnight vacuum at 80 °C. The $CuCo_2O_4$ electrodes were obtained after annealing the as-prepared electrode at 350 °C for 2 h (ramp rate of 5 °C/min) in the air. The electrodes were termed as $CuCo_2O_4$-1, $CuCo_2O_4$-2, and $CuCo_2O_4$-3 based on the solvent composition of 100 vol% water, 50/50 vol% water/ethanol, and 100 vol% ethanol, respectively.

Secondly, copper cobalt sulfide was prepared by dissolving 50 mg of thioacetamide in 20 ml of ethanol to form a homogeneous solution. The solution was then transferred to a Teflon autoclave reactor containing precursor Ni-foams from the previous step. The reaction was carried out at 160 °C for 6 h. As similar to an aforementioned procedure, the precipitates and electrodes were washed several times with ethanol and dried under vacuum at 80 °C overnight. The final electrodes are termed as $CuCo_2S_4$-1, $CuCo_2S_4$-2, and $CuCo_2S_4$-3, corresponding to the solvents used such as 100 vol% water, 50/50 vol% water/ethanol, and 100 vol% ethanol, respectively for their synthesis. The weight of material over the electrode was ~2 mg/cm^2.

The structural identity, phase purity and physical morphology of all the fabricated electrodes were analyzed using X-ray diffraction (XRD) and scanning electron microscopy (SEM). Cu$K\alpha_1$ ($\lambda = 1.5406$ Å) radiation was used to record the X-ray diffraction patterns in 2θ-θ mode. The sample morphology was characterized by scanning electron microscopy (SEM, JEOL JSM-840A).

Electrochemical measurements for energy generation and storage were performed using Versastat 4–500 electrochemical workstation (Princeton Applied Research, USA). The study was carried out using three-electrode and two-electrode system. The synthesized $CoCu_2O_4$ and $CoCu_2S_4$ electrodes were directly used as a working electrode. A platinum wire and saturated calomel

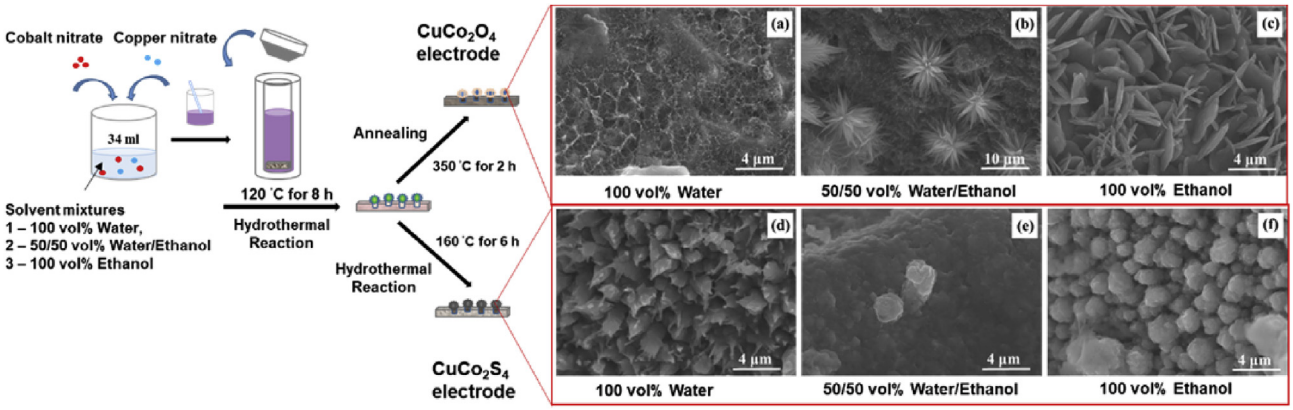

Fig. 1. Scheme for the synthesis and application of $CuCo_2S_4$ electrodes.

electrode (SCE) were used as counter and reference electrodes, respectively. All the experiments for electrocatalysis and energy storage were performed using 1M and 3M KOH electrolyte, respectively. Electrocatalytic properties of the synthesized electrodes were studied using linear sweep voltammetry (LSV), cyclic voltammetry (CV) and chronoamperometry (CA). While the charge storage performance was measured using cyclic voltammetry and galvanostatic charge-discharge (CD). LSV was performed at a scan rate of 2 mV/s for both OER and HER measurements. The potential was converted to RHE using the Nernst equation [19]. Electrochemical impedance spectroscopic (EIS) was performed during all the tests in the frequency range of 0.05 Hz−10 kHz with an applied AC amplitude of 10 mV.

3. Results and discussion

In this study, the nanostructured morphology of $CuCo_2O_4$ and $CuCo_2S_4$ were tailored using different solvent mixtures. The synthesis of $CuCo_2O_4$ using 100 vol% water, 50/50 vol% water/ethanol and 100 vol% ethanol resulted in the porous film, nanoneedle flower and porous petal type of morphology as observed from the SEM images in Fig. 1(a–c). Similar behavior of change in nano-morphology was observed for $CuCo_2S_4$ and summarized in Fig. 1(d–f). Although nano-morphology of multinary Cu-Co system resulted in different structures, their phase purity and crystalline nature showed identical behavior. The dependence of the morphology on the solvent could be due to the difference in the polarity of the solvent. The polarity of ethanol is lower than water. The solvent with high ethanol/water ration has a lower polarity than pure water. The effect of solvent polarity on the morphology of the synthesized materials was also observed in different materials [22–24]. The powder XRD patterns for $CuCo_2O_4$ in Fig. 2(a) corresponds to pure cubic spinel phase of $CuCo_2O_4$ (JCPDS card no. 78-2177) [25]. In addition, no other impurity peaks were observed, suggesting the high purity of the material. The diffraction peaks of $CuCo_2S_4$ samples in Fig. 2(b) can be indexed to polycrystalline $CuCo_2S_4$ that match very well with the JCPDS card no. 42-1450, with no oxide impurity phase indicating total conversion of $CuCo_2O_4$ to $CuCo_2S_4$ [19,26]. The $CuCo_2S_4$ samples show lower peaks intensities compared to $CuCo_2O_4$ samples with an amorphous background.

The average crystallite size (t) was calculated using the Debye–Scherrer's equation, $t = 0.9\lambda/\beta\cos\theta$, where λ is the X-ray wavelength, β is the full width at half maximum of the diffraction line, and θ is the diffraction angle of the XRD spectra [27]. The average crystallite size was calculated to be 14.4, 13.8, 16.7, 17.1, 14.4 and 18.4 nm for $CuCo_2O_4$-1, $CuCo_2O_4$-2, $CuCo_2O_4$-3, $CuCo_2S_4$-1, $CuCo_2S_4$-2, and $CuCo_2S_4$-3, respectively. The Williamson-Hall relationship was used to estimate percentage strain in the synthesized samples [28,29]. The percentage strain in the particles was estimated to be 0.74, 0.77, 0.89, 0.31, 0.37 and 0.30 for $CuCo_2O_4$-1, $CuCo_2O_4$-2, $CuCo_2O_4$-3, $CuCo_2S_4$-1, $CuCo_2S_4$-2, and $CuCo_2S_4$-3, respectively.

The electrocatalytic performance of $CuCo_2O_4$ and $CuCo_2S_4$ as an oxygen evolution catalyst was investigated using the LSV test. The polarization curves for the synthesized samples are shown in Fig. 3(a and b). The $CuCo_2O_4$-3 showed the lowest overpotential of 325 mV at 10 mA/cm^2 compared to $CuCo_2O_4$-1 (371 mV) and $CuCo_2O_4$-2 (371 mV). Increased concentration of ethanol during the synthesis greatly enhances the electrochemical performance of the metal oxides [30]. These results were further improved after sulfurization of the samples. The oxidation peak around 1.4 V can be ascribed to Ni(II) to Ni(III) [31,32]. The electrocatalytic performance of the $CuCo_2S_4$-3 sample showed the lowest overpotential of 290 mV at a current density of 20 mA/cm^2. This could be attributed to the nanoporous morphology of $CuCo_2S_4$-3 obtained using ethanol during the synthesis which provides enhanced electrocatalytic performance. The electrochemical surface area of $CuCo_2O_4$ and $CuCo_2S_4$ was estimated using CV in the non-Faradic region. A linear relationship between current density and scan rate of the synthesized samples was observed. The slope of the curve provides the value of double layer capacitance which is directly related to the surface area of these materials [33]. Double layer capacitance of 0.28 and 9.5 mF/cm^2 was calculated for $CuCo_2O_4$ and $CuCo_2S_4$, respectively (Fig. S1). Among the $CuCo_2S_4$ samples, the electrochemical surface area was observed to be 5.7, 8.1 and 9.5 mF/cm^2 for $CuCo_2S_4$-1, $CuCo_2S_4$-2, and $CuCo_2S_4$-3, respectively (Fig. S1). Although among the oxides and sulfides samples, oxides showed higher electrochemical surface area, their high impedance and larger charge transfer resistance counterbalance their catalytic effects (Fig. S2).

The observed results were comparable to previously reported multinary catalyst systems in alkaline media and summarized in Table S1. Reaction kinetics was studied using Tafel slopes (Fig. S3). The long-term durability of $CuCo_2S_4$-3 electrode was performed using cyclic stability test and chronoamperometry test. The electrochemical stability of the electrode was also studied under various bending test. The polarization curves for $CuCo_2S_4$-3 during stability test after 2,000th cycles and bending test from 0° to 60° showed stable behavior (Fig. 3(c and d)). Moreover, the chronoamperometry test showed stable values for the resulting current under constant applied potential for 17 h, suggesting the stable longterm performance of the electrode (Fig. S4).

The electrochemical performance of $CuCo_2S_4$ was further

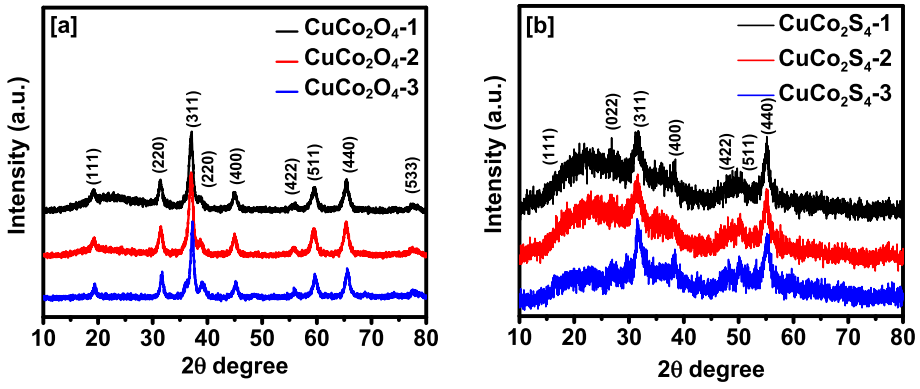

Fig. 2. XRD pattern of the synthesized (a) $CuCo_2O_4$ and (b) $CuCo_2S_4$ samples.

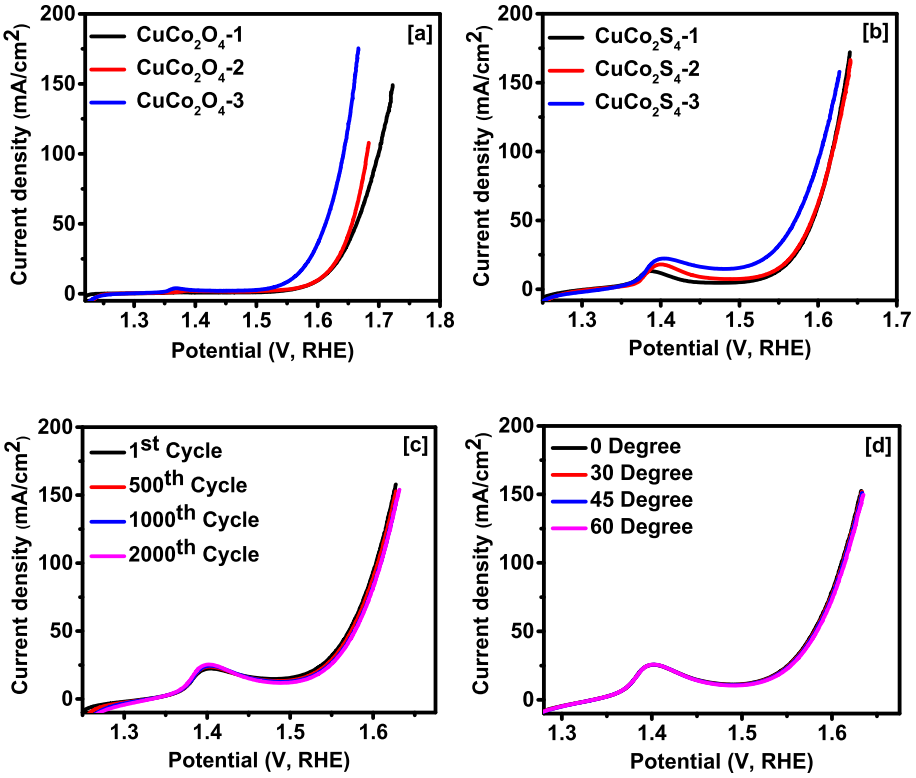

Fig. 3. Results for catalytic performance in OER test. Polarization curves for (a) $CuCo_2O_4$ and (b) $CuCo_2S_4$; (c) LSV stability test for $CuCo_2S_4$-3, and (d) Bending test for $CuCo_2S_4$-3.

investigated as an electrocatalyst for HER. The electrocatalytic performance of $CuCo_2S_4$ as HER catalyst followed the similar trend for overpotential results as observed in the OER test. The $CuCo_2S_4$-3 sample showed the lowest overpotential of 158 mV at 10 mA/cm^2 and Tafel slope of 113 mV/dec suggesting higher electrocatalytic performance for HER process (Fig. 4(b)). Lower Tafel slope suggest faster reaction kinetics for producing hydrogen gas. The observed overpotential and Tafel slope of $CuCo_2S_4$-3 for HER reaction were comparable to previous reports for HER electrocatalysts and can be observed from Table S2. Furthermore, the durability performance using cyclic stability for 2000 cycles and chronoamperometry test for 20 h showed stable catalytic performance (Fig. S5). This suggests that $CuCo_2S_4$ could serve as a promising material for HER catalysis.

The bifunctional electrocatalytic performance of $CuCo_2S_4$ was analyzed using a two-electrode system. The electrolyzer cell was fabricated using two symmetrical electrodes of $CuCo_2O_4$ and $CuCo_2S_4$ to study overall water splitting. The polarization curves in Fig. 5(a) shows higher electrocatalytic performance for the symmetrical $CuCo_2S_4$-3 cell as compared to the symmetrical $CuCo_2O_4$-3 cell. The symmetrical $CuCo_2S_4$-3 cell and $CuCo_2O_4$-3 cell required the potential of 1.66 and 1.77 V to obtain the current density of 10 mA/cm^2, respectively. The chronoamperometry test showed stable electrolysis for more than 24 h suggesting superior stability of the synthesized electrodes (Fig. 5(b)).

The effect of solvent over the charge storage performance of the synthesized material was analyzed using cyclic voltammetry and galvanostatic charge-discharge test. The CV test showed obvious improvement in total area under the CV curve for synthesized $CuCo_2O_4$-3 and $CuCo_2S_4$-3 samples compared to the other two samples (Fig. S6(a and c)). This improvement was consistent with longer discharge time observed in galvanostatic charge-discharge curves in Fig. S6(b and d). Significant improvement was observed in specific capacitance values of $CuCo_2S_4$ electrodes, after sulfurization of the $CuCo_2O_4$ electrodes (Fig. 6(a and b)). The $CuCo_2S_4$-3 electrode showed improved specific capacitance values to 6.3 F/cm^2 (3190.8 F/g) as compared to $CuCo_2O_4$ (0.57 F/cm^2 or 285.5 F/g) at

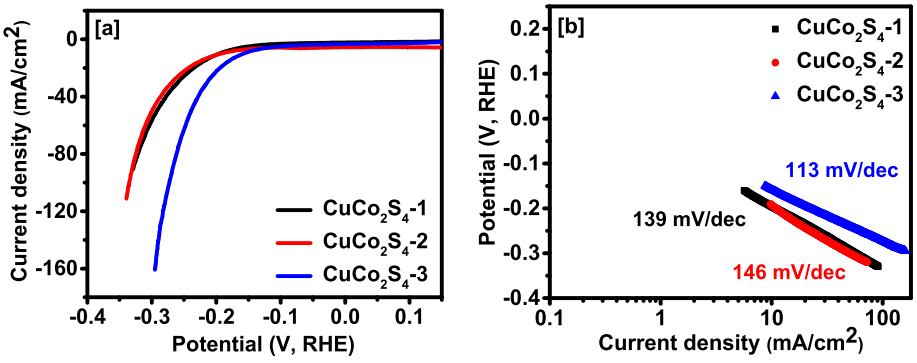

Fig. 4. Results for the catalytic performance of $CuCo_2S_4$ in HER test. (a) Polarization curves, and (b) Tafel slope.

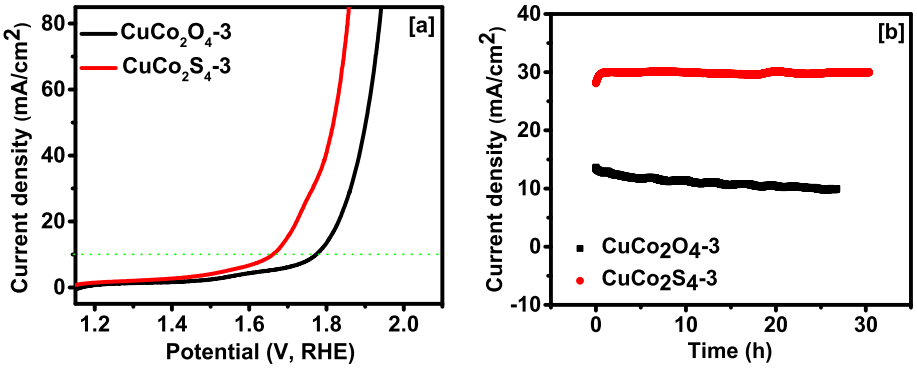

Fig. 5. (a) Polarization and (b) Chronoamperometry plots for overall water splitting of a two-electrode electrolyzer.

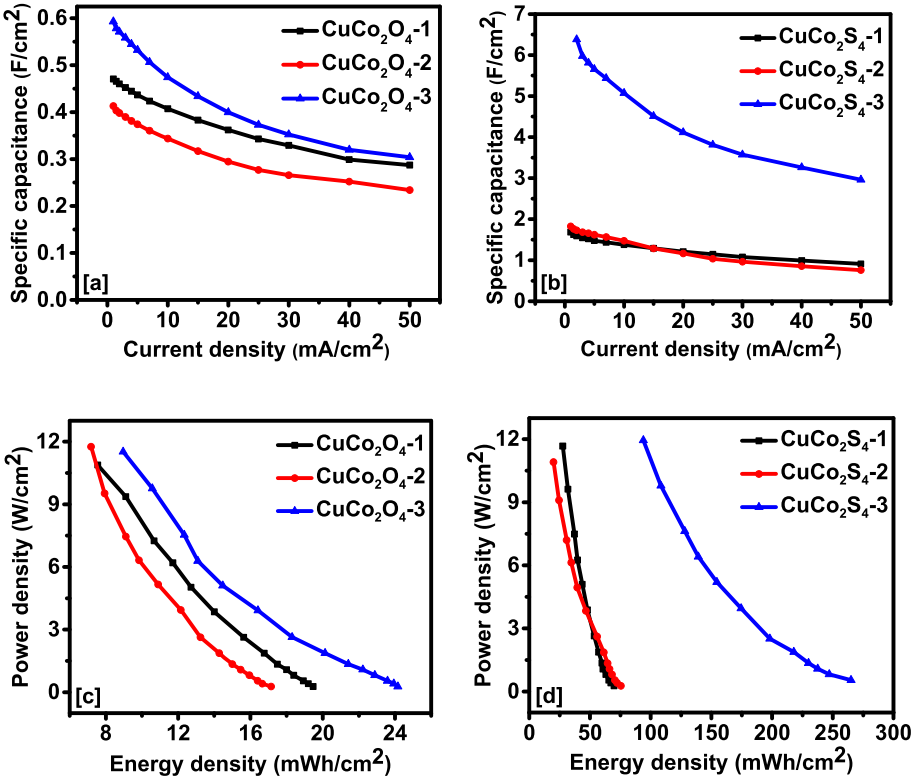

Fig. 6. Specific capacitance vs current density of (a) $CuCo_2O_4$ and, (b) $CuCo_2S_4$; Ragone plot for (c) $CuCo_2O_4$ and, (d) $CuCo_2S_4$.

current density of 2 mA/cm^2. The obtained results were higher compared to previously reported supercapacitor electrodes (Table S3). The areal energy and power densities of the synthesized electrodes can be outlined using Ragone plot (Fig. 6(b and c)). The energy and power densities for $CuCo_2S_4$-3 were observed to be 265 mWh/cm^2 (132 Wh/kg) and 11.9 W/cm^2 (5973 W/kg), respectively. The observed values were higher compared to all previously reported multinary $CuCo_2S_4$ system and summarized in Table S4. Wei et al. have synthesized $CuCo_2O_4$@ carbon quantum dots (CQDs) for overall water splitting and supercapacitor applications [17,34]. The asymmetrical supercapacitors made of 3D porous hierarchical $CuCo_2O_4$@carbon quantum dots (CQDs) and Fe_2O_3@CQDs showed an energy density of 39.5 Wh/kg at 1203.7 W/kg [34]. Higher energy density and power density of $CuCo_2S_4$ could enable its potential applicability in advanced energy storage systems such as batteries for efficient and safer operations [35,36]. For example, Ji et al. fabricated novel dual ion battery and observed energy density of 155 Wh/kg at a power density of 116 W/kg [37]. Although batteries provide higher energy density, they lack to provide higher power density and thereby, lack to serve the purpose of high power in the electric motor vehicle when used alone [38,39]. Hence, utilizing $CuCo_2S_4$ described in this work could serve as an efficient alternative high power energy storage system. Moreover, cyclic stability test for 5000 cycles using $CuCo_2O_4$ and $CuCo_2S_4$ electrodes showed capacitance retention of 100% (Fig. S7(a and b)). Both the electrodes maintained the Coulombic efficiency of about 100% suggesting efficient charge storage behavior. The overall study suggests that $CuCo_2S_4$-3 sample could be used as an efficient electrode for high-performance supercapacitors.

4. Conclusions

Tailoring the nanomorphology of electrochemically active materials such as $CuCo_2O_4$ and $CuCo_2S_4$, by using different vol% of

water and ethanol could result in different nano-shapes and affect the final energy generation and storage properties. The electrocatalytic performance of $CuCo_2S_4$ for HER and OER process resulted in a low overpotential requirement of 158 mV to reach 10 mA/cm^2 and 290 mV at 20 mA/cm^2, respectively with high cyclic stability. The overall water-splitting using an electrolyzer cell with symmetrical electrodes of $CuCo_2S_4$ showed a low cell potential of 1.66 V at 10 mA/cm^2 with long cycling lifespan. The $CuCo_2S_4$ electrode displayed ultra-high areal capacitance of 6.3 F/cm^2 (3190.8 F/g) at 2 mA/cm^2 with areal energy and power densities of 265 mWh/cm^2 (132 Wh/kg) and 11.9 W/cm^2 (5973 W/kg), respectively. The results were comparable to advanced battery systems and suggest great potential of $CuCo_2S_4$ for green energy production and storage.

Author contributions

RKG conceived the project, designed the experiments, interpreted the data, and finalized the manuscript. The first draft of the manuscript was written by CZ and SB. CZ performed all the electrochemical measurements. FW and XL provided SEM images. All authors reviewed and commented on the manuscript.

Acknowledgments

Dr. Ram K. Gupta expresses his sincere acknowledgment to the Polymer Chemistry Program and the Kansas Polymer Research Center, Pittsburg State University for providing financial and research support to complete this project. XL wants to thank the financial support from General Research Fund provided by the University of Kansas and funding support from NSF (1833048).

Appendix A. Supplementary data

Supplementary data to this article can be found online at https://doi.org/10.1016/j.jallcom.2019.01.012.

References

[1] C. Zequine, S. Bhoyate, K. Siam, P.K. Kahol, N. Kostoglou, C. Mitterer, S.J. Hinder, M.A. Baker, G. Constantinides, C. Rebholz, G. Gupta, X. Li, R.K. Gupta, Needle grass array of nanostructured nickel cobalt sulfide electrode for clean energy generation, Surf. Coating. Technol. 354 (2018) 306–312.
[2] C. Zhang, S. Bhoyate, M. Hyatt, B.L. Neria, K. Siam, P.K. Kahol, M. Ghimire, S.R. Mishra, F. Perez, R.K. Gupta, Nitrogen-doped flexible carbon cloth for durable metal free electrocatalyst for overall water splitting, Surf. Coating. Technol. 347 (2018) 407–413.
[3] C. Zhang, Z. Wang, S. Bhoyate, T. Morey, B. Neria, V. Vasiraju, G. Gupta, S. Palchoudhury, P. Kahol, S. Mishra, F. Perez, R. Gupta, MoS_2 decorated carbon nanofibers as efficient and durable electrocatalyst for hydrogen evolution reaction C 3 (2017), 33(1)-33(12).
[4] C.K. Ranaweera, C. Zhang, S. Bhoyate, P.K. Kahol, M. Ghimire, S.R. Mishra, F. Perez, B.K. Gupta, R.K. Gupta, Flower-shaped cobalt oxide nano-structures as an efficient, flexible and stable electrocatalyst for the oxygen evolution reaction, Mater. Chem. Front. 1 (2017) 1580–1584.
[5] H. Adhikari, M. Ghimire, C.K. Ranaweera, S. Bhoyate, R.K. Gupta, J. Alam, S.R. Mishra, Synthesis and electrochemical performance of hydrothermally synthesized Co_3O_4 nanostructured particles in presence of urea, J. Alloys Compd. 708 (2017) 628–638.
[6] C. Coughlan, M. Ibáñez, O. Dobrozhan, A. Singh, A. Cabot, K.M. Ryan, Compound copper chalcogenide nanocrystals, Chem. Rev. 117 (2017) 5865–6109.
[7] M.D. Regulacio, Y. Wang, Z.W. Seh, M.-Y. Han, Tailoring porosity in copper-based multinary sulfide nanostructures for energy, biomedical, catalytic, and sensing applications, ACS Appl. Nano Mater. 1 (2018) 3042–3062.
[8] K. Ramasamy, H. Sims, S. Palchoudhury, S. Ivanov, A. Gupta, Layered ternary sulfide $CuSbS_2$ nanoplates for flexible solid- state supercapacitors, J. Mater. Chem. A 3 (2015) 13263–13274.
[9] K. Ramasamy, R.K. Gupta, S. Palchoudhury, S. Ivanov, A. Gupta, Layer-structured copper antimony chalcogenides ($CuSbSe_xS_{2-x}$): stable electrode materials for supercapacitors, Chem. Mater. 27 (2015) 379–386.
[10] Y. Li, J. Yin, L. An, M. Lu, K. Sun, Y.Q. Zhao, F. Cheng, P. Xi, Metallic $CuCo_2S_4$ nanosheets of atomic thickness as efficient bifunctional electrocatalysts for portable, flexible Zn-air batteries, Nanoscale 10 (2018) 6581–6588.
[11] S. Zhao, Y. Wang, Q. Zhang, Y. Li, L. Gu, Z. Dai, S. Liu, Y.Q. Lan, M. Han, J. Bao, Two-dimensional nanostructures of non-layered ternary thiospinels and their bifunctional electrocatalytic properties for oxygen reduction and evolution: the case of $CuCo_2S_4$ nanosheets, Inorg. Chem. Front. 3 (2016) 1501–1509.
[12] W. Xu, J. Lu, W. Huo, J. Li, X. Wang, C. Zhang, X. Gu, C. Hu, Direct growth of $CuCo_2S_4$ nanosheets on carbon fiber textile with enhanced electrochemical pseudocapacitive properties and electrocatalytic properties towards glucose oxidation, Nanoscale 10 (2018) 14304–14313.
[13] J. Tang, Y. Ge, J. Shen, M. Ye, Facile synthesis of $CuCo_2S_4$ as a novel electrode material for ultrahigh supercapacitor performance, Chem. Commun. 52 (2016) 1509–1512.
[14] A. Pendashteh, S.E. Moosavifard, M.S. Rahmanifar, Y. Wang, M.F. El-Kady, R.B. Kaner, M.F. Mousavi, Highly ordered mesoporous $CuCo_2O_4$ nanowires, a promising solution for high-performance supercapacitors, Chem. Mater. 27 (2015) 3919–3926.
[15] K. Chen, J. Zhou, W. Chen, Q. Zhong, T. Yang, X. Yang, C. Deng, Y. Liu, Growth kinetics and mechanisms of multinary copper-based metal sulfide nanocrystals, Nanoscale 9 (2017) 12470–12478.
[16] J. Huang, Y. Sun, Y. Zhang, G. Zou, C. Yan, S. Cong, T. Lei, X. Dai, J. Guo, R. Lu, Y. Li, J. Xiong, A new member of electrocatalysts based on nickel metaphosphate nanocrystals for efficient water oxidation, Adv. Mater. 30 (2018), 1705045(1)-1705045(7).
[17] G. Wei, J. He, W. Zhang, X. Zhao, S. Qiu, C. An, Rational design of Co(II) dominant and oxygen vacancy defective $CuCo_2O_4$@CQDs hollow spheres for enhanced overall water splitting and supercapacitor performance, Inorg. Chem. 57 (2018) 7380–7389.
[18] S.H. Guo, W.Q. Chen, M. Li, J. Wang, F. Liu, J.P. Cheng, Effect of reaction temperature on the amorphous-crystalline transition of copper cobalt sulfide for supercapacitors, Electrochim. Acta 271 (2018) 498–506.
[19] M. Chauhan, K.P. Reddy, C.S. Gopinath, S. Deka, Copper cobalt sulfide nanosheets realizing a promising electrocatalytic oxygen evolution reaction, ACS Catal. 7 (2017) 5871–5879.
[20] S. Czioska, J. Wang, X. Teng, Z. Chen, Hierarchically structured $CuCo_2S_4$ nanowire arrays as efficient bifunctional electrocatalyst for overall water splitting, ACS Sustain. Chem. Eng. 6 (2018) 11877–11883.
[21] X. Xu, Y. Liu, P. Dong, P.M. Ajayan, J. Shen, M. Ye, Mesostructured $CuCo_2S_4$/$CuCo_2O_4$ nanoflowers as advanced electrodes for asymmetric supercapacitors, J. Power Sources 400 (2018) 96–103.
[22] Y. Dong, K. He, L. Yin, A. Zhang, A facile route to controlled synthesis of Co_3O_4 nanoparticles and their environmental catalytic properties, Nanotechnology 18 (2007), 435602(1)- 435602(8).
[23] Y. Anil Kumar, S. Srinivasa Rao, D. Punnoose, C. Venkata Tulasivarma, C.V.V.M. Gopi, K. Prabakar, H.-J. Kim, Influence of solvents in the preparation of cobalt sulfide for supercapacitors, R. Soc. Open Sci. 4 (2017), 170427(1)-170427(11).
[24] S.J. Folkman, M. Zhou, M. Nicki, R.G. Finke, Alcohol solvent effects in the synthesis of Co_3O_4 metal-oxide nanoparticles: disproof of a surface-ligand thermodynamic effect en route to alternative kinetic and thermodynamic explanations, Inorg. Chem. 57 (2018) 1517–1526.
[25] H.S. Jadhav, S.M. Pawar, A.H. Jadhav, G.M. Thorat, J.G. Seo, Hierarchical mesoporous 3D flower-like $CuCo_2O_4$/NF for high-performance electrochemical energy storage, Sci. Rep. 6 (2016), 31120(1)- 31120(12).
[26] T. Wang, M. Liu, H. Ma, Facile synthesis of flower-like copper-cobalt sulfide as binder-free faradaic electrodes for supercapacitors with improved electrochemical properties, Nanomaterials 7 (2017), 140(1)-140(11).
[27] R.K. Gupta, K. Ghosh, L. Dong, P.K. Kahol, Green synthesis of hematite (α-Fe2O3) submicron particles, Mater. Lett. 64 (2010) 2132–2134.
[28] A. Bhattacharya, R.K. Gupta, P.K. Kahol, K. Ghosh, Electrical properties of rectifying contacts on selectively carrier controlled grown ZnO thin films, J. Appl. Phys. 108 (2010), 34514(1)-34514(5).
[29] R.K. Gupta, K. Ghosh, P.K. Kahol, Structural and magnetic properties of epitaxial $SnFe_2O_4$ thin films, Mater. Lett. 65 (2011) 2149–2151.
[30] L. Zhang, H. Gong, A cheap and non-destructive approach to increase coverage/loading of hydrophilic hydroxide on hydrophobic carbon for lightweight and high-performance supercapacitors, Sci. Rep. 5 (2015), 18108(1)-18108(11).
[31] Z. Pu, Y. Luo, A.M. Asiri, X. Sun, Efficient electrochemical water splitting catalyzed by electrodeposited nickel diselenide nanoparticles based film, ACS Appl. Mater. Interfaces 8 (2016) 4718–4723.
[32] J. Zhang, Y. Wang, C. Zhang, H. Gao, L. Lv, L. Han, Z. Zhang, Self-supported porous $NiSe_2$ nanowrinkles as efficient bifunctional electrocatalysts for overall water splitting, ACS Sustain. Chem. Eng. 6 (2018) 2231–2239.
[33] C.C.L. McCrory, S. Jung, J.C. Peters, T.F. Jaramillo, Benchmarking heterogeneous electrocatalysts for the oxygen evolution reaction, J. Am. Chem. Soc. 135 (2013) 16977–16987.
[34] G. Wei, X. Zhao, K. Du, Y. Huang, C. An, S. Qiu, M. Liu, S. Yao, Y. Wu, Flexible asymmetric supercapacitors made of 3D porous hierarchical $CuCo_2O_4$@CQDs and Fe_2O_3@CQDs with enhanced performance, Electrochim. Acta 283 (2018) 248–259.
[35] H. Zhu, F. Zhang, J. Li, Y. Tang, Penne-Like MoS_2/carbon nanocomposite as anode for sodium-ion-based dual-ion battery, Small 14 (2018), 1703951(1)-1703951(7).
[36] R. Schmuch, R. Wagner, G. Hörpel, T. Placke, M. Winter, Performance and cost of materials for lithium-based rechargeable automotive batteries, Nat. Energy 3 (2018) 267–278.

[37] B. Ji, F. Zhang, X. Song, Y. Tang, A novel potassium-ion-based dual-ion battery, Adv. Mater. 29 (2017), 1700519(1)- 1700519(7).
[38] H. Budde-Meiwes, J. Drillkens, B. Lunz, J. Muennix, S. Rothgang, J. Kowal, D.U. Sauer, A review of current automotive battery technology and future prospects, Proc. Inst. Mech. Eng. - Part D J. Automob. Eng. 227 (2013) 761–776.
[39] A. Burke, H. Zhao, Present and future applications of supercapacitors in electric and hybrid vehicles, in: 2015 IEEE 82nd Veh. Technol. Conf., IEEE, 2015, p. 5.